

Luminescent and Raman Active Silver Nanoparticles with Polycrystalline Structure

Jie Zheng,^{*,†,‡,⊥} Yong Ding,[§] Bozhi Tian,[†] Zhong Lin Wang,[§] and Xiaowei Zhuang^{†,‡,¶}

Department of Chemistry and Chemical Biology, Howard Hughes Medical Institute, Harvard University, Cambridge, Massachusetts 02138, School of Material Science and Engineering, Georgia Institute of Technology, Atlanta, Georgia 30332, and Department of Physics, Harvard University, Cambridge, Massachusetts 02138

Received May 3, 2008; E-mail: jiezheng@fas.harvard.edu

Noble metal nanostructures on different length scales exhibit a variety of optical properties ranging from plasmon resonance¹ and Raman enhancement² to fluorescence,³ providing novel opportunities for bioimaging and sensing.⁴ In a regime where the particle size is on the same order of the electron Fermi wavelength (~ 0.5 nm for silver and gold), metal nanoparticles (NPs) often display strong single-electron excitations and emit fluorescence.³ However, as particle size approaches electron mean free path length (~ 50 nm for silver and gold), fluorescence usually disappears and, instead, collective excitations of electrons become dominant, leading to plasmon resonance. Large Raman enhancements have also been observed from nanoclusters⁵ and NPs⁶ of noble metals. It has been shown recently that electron–phonon interactions within metal NPs can be modified by the crystallinity.⁷ Thus, control of the particle size and structure is a powerful strategy to modulate electronic structures and optical properties of metal NPs. Here, we report the observation that polycrystalline silver NPs with grain sizes down to electron Fermi wavelength exhibit both bright luminescence and a large enhancement effect on the Raman scattering signals of proximal molecules (an effect being referred to as “Raman activity” hereafter). The number of photons emitted from these NPs exceeded that from quantum dots or dye molecules by approximately 2 or 5 orders of magnitude, respectively.

We synthesized luminescent and Raman active metal NPs by thermal reduction of silver ions in glycine matrix, taking advantage of the solid-state matrix to control the nucleation and migration of reduced silver atoms (see Supporting Information (SI) for synthesis protocol). The glycine-coated NPs remained stable in aqueous solution for more than 2 years at ambient conditions (Figure 1a). Transmission electron microscopy (TEM) revealed particle diameters ranging from 2 to 30 nm. Different size fractions of NPs can be separated using centrifugation (see SI). TEM images of two such fractions, with particle diameters of 18 ± 3 and 3 ± 1 nm, are shown in Figure 1a and Figure S1a–c.

Luminescence from these NPs can be readily detected at the single-particle level. Comparison of the Rayleigh scattering (dark field) and luminescence images showed that more than 95% of the NPs were luminescent (Figure 1b). This was in contrast to colloidal silver NPs prepared by typical solution-phase methods, of which only $\sim 2\%$ of the particles emit luminescence (Figure S2). TEM characterization indicated that the great majority of the NPs appear as individual particles rather than aggregates (Figure S3). These NPs created by solid-phase synthesis are remarkably bright and photostable; under the same excitation conditions, the half-lifetime of the 18 nm silver NPs was 660 s, while the half-lifetimes of the Rhodamine 6G (R6G)

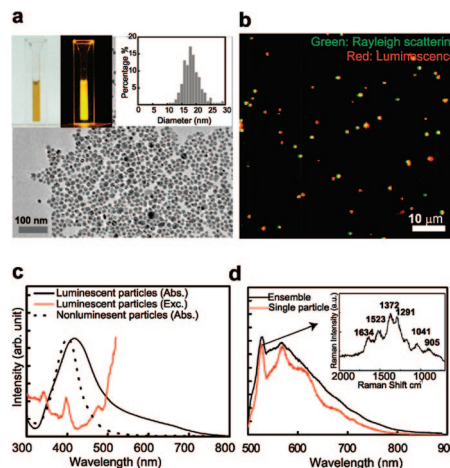


Figure 1. Solid-phase synthesis creates silver NPs with bright and robust luminescence. (a) Upper left panel: An aqueous solution of the 18 nm glycine-coated silver NPs. The photos were taken without (left) and with (right) 532 nm laser excitation; in the latter case, a 545 nm long pass filter was used to block the scattered laser light. Lower panel: TEM image of the NPs. Upper right panel: Size distribution of the NPs determined from TEM. (b) An overlay Rayleigh scattering (green) and luminescent (red) image of the NPs. NPs with yellow or orange color exhibit both luminescent and Rayleigh scattering. (c) Absorption (solid black) and excitation (red) spectra of the luminescent silver NPs. As a comparison, the black dashed line shows the absorption of the 20 nm nonluminescent silver NPs produced by solution-phase synthesis. (d) Ensemble (black) and single-particle (red) emission spectra of luminescent silver NPs. Inset: using a high-density grating, the Raman peak of the single-particle emission spectrum was further resolved into multiple lines.

molecules and the commercially available quantum dots (CdSe/ZnS core–shell, emission maximum at 605 nm) were only 0.4 and 37 s, respectively (Figure S4). The average luminescence intensity from individual silver NPs was 40 and 4 times larger than those from single R6G molecules and quantum dots, respectively. Thus the total number of photons emitted from individual silver NPs is nearly 70 000 times larger than that from R6G molecules and nearly 70 times larger than that from quantum dots. Using the previously determined number of photons emitted from R6G ($\sim 10^6$),⁸ we estimated that a single silver NP emitted on average 7×10^{10} photons before photobleaching. The average number of photons emitted from the 3 nm silver NPs was estimated to be 4×10^9 using a similar approach (Figure S1d).

To further explore the optical properties of these NPs, we measured the absorption, excitation, and emission spectra of the 18 nm NPs, which can be readily produced in high concentration to allow ensemble spectral characterization. The absorption spectrum displayed a peak near the plasmon resonance of nonluminescent silver NPs, but with a significantly broader width (Figure 1c, black line), suggesting the possible presence of additional optical transitions besides plasmons.¹ The excitation spectrum adopted an almost opposite trend, exhibiting

[†] Department of Chemistry and Chemical Biology, Harvard University.

[‡] Howard Hughes Medical Institute, Harvard University.

[§] Georgia Institute of Technology.

[¶] Department of Physics, Harvard University.

[⊥] Present address: Department of Chemistry, The University of Texas at Dallas. E-mail: jiezheng@utdallas.edu.

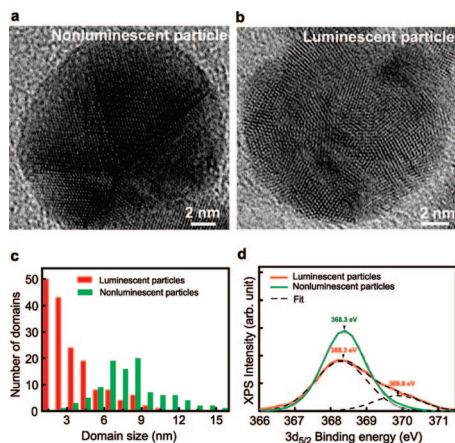


Figure 2. Structural characterizations of silver NPs by HRTEM. TEM images of a nonluminescent NP created by solution-phase synthesis (a) and a luminescent NP created by solid-phase synthesis (b). (c) Domain size distributions obtained from luminescent (red) and nonluminescent (green) NPs. In each case, 15 NPs were characterized. Domain sizes were measured as the average of the long and short axes of the individual domains. (d) X-ray photoelectron spectra (XPS) of luminescent and nonluminescent silver NPs. The spectrum of the nonluminescent NPs (green) was fit to a Gaussian centered at 368.3 eV (gray dashed line). The spectrum of the luminescent NPs (red) was fit with two Gaussians centered at 369.9 and 368.3 eV, respectively (black dashed lines).

a minimum at the absorption peak (Figure 1c, red line), and multiple narrow peaks were also found to superimpose on the broad trend of the excitation spectrum. These observations suggest that plasmons do not make major contributions to the luminescence, rather the luminescence likely arises from single-electron excitations between discrete energy states.¹ The luminescence spectra of individual NPs exhibited a narrow peak superimposed on a broadband (Figure 1d). The frequency difference between the sharp peak and the excitation wavelength is independent of the excitation wavelength, indicative of its Raman scattering nature (Figure S5). The Raman peak can be further resolved into multiple lines (Figure 1d inset), some of which are close to the previous reported surface enhanced Raman spectra (SERS) of glycine⁹ (Figure S6). Therefore, the enhancement effect due to these silver NPs allows the Raman scattering signal of glycine-coated molecules on individual NPs to be readily detected. To obtain a rough estimate of the Raman enhancement factor, we assumed that every silver atom on the 18 nm particle was bound to a glycine molecule and obtained a lower limit estimate of 10^{10} for the enhancement factor (see SI for details). The Raman peak positions and intensities of the individual particle fluctuated over time, and heterogeneity among particles was also observed (Figure S6). While the Raman signal was encoded with chemical information of glycine, the broad luminescence band from the silver NPs did not appear to require a specific glycine coating. With the same synthetic strategy, we also created acetate-coated silver NPs, which also exhibited a broad luminescence band but different Raman signature (Figure S7).

To investigate potential material structures responsible for the observed optical properties, we used high-resolution TEM to probe structural differences between the luminescent silver NPs created by solid-phase synthesis and the nonluminescent silver particles of similar sizes (~ 20 nm) produced by solution-phase synthesis. The nonluminescent NPs typically showed single-crystalline or twinned structures with domain sizes averaging around 8 nm (Figure 2a,c). In contrast, the luminescent NPs displayed a polycrystalline structure with numerous small domains. The domain sizes were primarily in the 1–2 nm range (Figure 2b,c). As an alternative approach to probe the domain size, we measured the binding energy (BE) of silver $3d_{5/2}$ electrons for both nonluminescent and luminescent NPs using X-ray photoelec-

tron spectroscopy (Figure 2d). The BE spectrum of the nonluminescent NPs showed predominantly a single peak at 368.3 eV, agreeing quantitatively with the bulk value for silver (368.1 eV).^{10a} In contrast, the spectrum of the luminescent NPs contained an additional peak at 369.9 eV, which is 1.8 eV blue-shifted from the bulk silver value. According to the previously determined correlation between the electron BE of silver and the particle size,^{10b} the blue shift corresponds to an average domain size of 0.9 nm. We note that the BE of the $3d_{5/2}$ electrons of silver oxides are in the range of 367.3 to 368.4 eV^{10c} and cannot explain the blue-shifted 369.9 eV peak. The small domains present in the NPs likely result in discrete energy states that give rise to optical transitions, and different sized subnanometer domains may result in different emission wavelengths (Figure 1d), consistent with size-dependent luminescence from small silver clusters.³ Previous calculations indicate that subnanometer silver clusters and their junctions can give rise to a very large Raman enhancement due to a combination of electromagnetic field enhancement and chemical enhancement effect.¹¹ Thus strong Raman enhancement may arise from the observed granular structure which contains many small domains and domain junctions.

In summary, we have created a new class of multidomain silver nanostructures with individual domain sizes down to 1 nm or less using a simple solid-phase thermal reduction method. These NPs exhibit exceedingly bright luminescence and strongly enhanced Raman scattering. These optical properties potentially allow the NPs to function as new probes for bioimaging.

Acknowledgment. This work was supported in part by NSF (to X.Z.), the NSF NSEC center at Harvard, and Emory–Georgia Tech Center for Cancer Nanotechnology of Excellence from NIH to (Z.L.W.). X.Z. is a Howard Hughes Medical Institute investigator. Authors sincerely thank Professor Charles M. Lieber at Harvard University for insightful discussions and suggestions.

Supporting Information Available: Detailed information for synthesis and characterizations of luminescent and Raman active silver NPs and supplementary figures. This material is available free of charge via the Internet at <http://pubs.acs.org>.

References

- (1) Kreibitz, U.; Vollmer, M. *Optical Properties of Metal Clusters*; Springer: Berlin, 1995; Vol. 25.
- (2) (a) Haynes, C. L.; McFarland, A. D.; Van Duyne, R. P. *Anal. Chem.* **2005**, *77*, 338A–346A. (b) Moskovits, M. *J. Raman Spectrosc.* **2005**, *36*, 485–496.
- (3) (a) Fedrigo, S.; Harbich, W.; Buttet, J. *J. Chem. Phys.* **1993**, *99*, 5712–5717. (b) Peyser, L. A.; Vinson, A. E.; Bartko, A. P.; Dickson, R. M. *Science* **2001**, *291*, 103–106. (c) Zheng, J.; Dickson, R. M. *J. Am. Chem. Soc.* **2002**, *124*, 13982–13983.
- (4) Mirkin, C. A.; Letsinger, R. L.; Mucic, R. C.; Storhoff, J. J. *Nature* **1996**, *382*, 607–609. (b) Sonnichsen, C.; Reinhard, B. M.; Liphardt, J.; Alivisatos, A. P. *Nat. Biotechnol.* **2005**, *23*, 741–745. (c) Qian, X. M.; Peng, X. H.; Ansari, D. O.; Yin-Goen, Q.; Chen, G. Z.; Shin, D. M.; Yang, L.; Young, A. N.; Wang, M. D.; Nie, S. M. *Nat. Biotechnol.* **2008**, *26*, 83–90.
- (5) Capadonna, L. P.; Zheng, J.; Gonzalez, J. I.; Lee, T. H.; Patel, S. A.; Dickson, R. M. *Phys. Rev. Lett.* **2005**, *94*.
- (6) (a) Nie, S. M.; Emery, S. R. *Science* **1997**, *275*, 1102–1106. (b) Kneipp, K.; Wang, Y.; Kneipp, H.; Perelman, L. T.; Itzkan, I.; Dasari, R.; Feld, M. S. *Phys. Rev. Lett.* **1997**, *78*, 1667–1670. (c) Jiang, J.; Bosnick, K. A.; Maillard, M.; Brus, L. E. *J. Phys. Chem. B* **2003**, *107*, 9964–9972. (d) Fromm, D. P.; Sundaramurthy, A.; Kinkhabwala, A.; Schuck, P. J.; Kino, G. S.; Moerner, W. E. *J. Chem. Phys.* **2006**, *124*.
- (7) Tang, Y.; Min, O. Y. *Nat. Mater.* **2007**, *6*, 754–759.
- (8) Moerner, W. E.; Fromm, D. P. *Rev. Sci. Instrum.* **2003**, *74*, 3597–3619.
- (9) (a) Suh, J. S.; Moskovits, M. *J. Am. Chem. Soc.* **1986**, *108*, 4711–4718. (b) Dou, X. M.; Jung, Y. M.; Cao, Z. Q.; Ozaki, Y. *Appl. Spectrosc.* **1999**, *53*, 1440–1447.
- (10) (a) Luo, K.; St Clair, T. P.; Lai, X.; Goodman, D. W. *J. Phys. Chem. B* **2000**, *104*, 3050–3057. (b) Wertheim, G. K.; Dicenzo, S. B. *Phys. Rev. B* **1988**, *37*, 844–847. (c) Database, NIST, XPS; <http://srdata.nist.gov/xps/>.
- (11) (a) Zhao, L. L.; Jensen, L.; Schatz, G. C. *J. Am. Chem. Soc.* **2006**, *128*, 2911–2919. (b) Zhao, L. L.; Jensen, L.; Schatz, G. C. *Nano Lett.* **2006**, *6*, 1229–1234.

JA803302P